Spectator electromagnetic effect on charged pion spectra in peripheral ultrarelativistic heavy ion collisions

Andrzej Rybicki
Henryk Niewodniczański Institute of Nuclear Physics, Polish Academy of Sciences, PL-31-342 Kraków, Poland

Antoni Szczurek
Henryk Niewodniczański Institute of Nuclear Physics, Polish Academy of Sciences, PL-31-342 Kraków, Poland and University of Rzeszów, PL-35-959 Rzeszów, Poland

(Received 10 October 2006; published 4 May 2007)

We estimate the electromagnetic effect of the spectator charge on the momentum spectra of π^+ and π^- produced in peripheral Pb+Pb collisions at energies currently available at the CERN Super Proton Synchrotron. We find that the effect is large and results in strongly varying structures in the x_F dependence of the π^+/π^- ratio, especially at low transverse momenta where a deep valley in this ratio is predicted at $x_F \sim 0.15-0.20$. It appears that the effect depends on initial conditions, i.e., on the time of initial pion emission, on the distance between the pion formation zone and the two spectator systems, and on the size of the pion emission source. Thus, it provides new information on the space and time evolution of the nonperturbative pion creation process.

DOI: 10.1103/PhysRevC.75.054903 PACS number(s): 12.38.Mh, 25.75.−q

I. MOTIVATION

The process of pion production in high energy hadronic reactions (like p+p, p+nucleus or nucleus+nucleus collisions) belongs to the domain of the strong interaction theory: quantum chromodynamics (QCD). For an enormous majority of pions produced, the mechanism underlying this process is nonperturbative. Here, QCD does not lead to quantitative predictions. Instead, phenomenological models are used [1]. These contain arbitrary scenarios of the hadronic collision dynamics and evidently rely on experimental input to differentiate right scenarios from wrong ones.

Most of the experimental input collected so far (at ISR, SPS, RHIC, and others) provides information exclusively about final state momentum space (p_x, p_y, p_z). Observables such as inclusive distributions of kinematical variables, or their correlations, give no information on how the reaction occurs in position space (x, y, z) or in time (t). To get such information, a specific phenomenon directly dependent on the reaction evolution in space and time has to be isolated. The Hanbury Brown-Twiss (HBT) effect [2] can be quoted as an example of such a phenomenon.

This paper considers another possible candidate for such a phenomenon in ultrarelativistic heavy ion collisions. We mean here the electromagnetic interaction between the remnants of the two nuclei (spectator systems) and the positive and negative pions produced in the course of the collision. The two highly charged spectator systems moving at relativistic velocities generate a rapidly changing electromagnetic field which modifies the original pion trajectories. This causes a distortion of observed kinematical pion spectra. It is to be expected that this distortion is interrelated to the dynamics of the collision and in particular to the time evolution and initial conditions of the participant and spectator zones.

Our aim is to study this electromagnetic "Coulomb" effect for the specific case of peripheral Pb+Pb collisions at energies currently available at the CERN Super Proton Synchrotron (SPS) (158 GeV/nucleon beam energy, $\sqrt{s_{NN}} = 17$ GeV). We choose peripheral collisions because they are characterized by the largest spectator charge. Our specific tasks are to (1) provide a general description of the main features of the effect in the framework of a simplified but realistic relativistic two-spectator model, (2) define the regions of produced pion phase space that are particularly sensitive to the electromagnetic influence of the two spectator systems, and (3) get a first idea on whether the electromagnetic effect depends on the evolution of the pion production process in space and time.

Seen in a more general context, our analysis is complementary to various studies of the role of specific phenomena such as multiple collisions [3], isospin effects [4], the neutron halo [5], or Fermi motion [6] in particle production in heavy ion reactions. To understand the role played by all these effects seems to us a necessity if a realistic description of the nonperturbative heavy ion collision dynamics is to be provided.

The remainder of this paper is organized as follows. The general context of Coulomb interactions in nuclear collisions is briefly discussed in Sec. II. The general idea and the details of our model are described in Sec. III. The results of our study are presented in Sec. IV. Conclusions are formulated in Sec. V.

II. COULOMB EFFECTS AT LOW AND HIGH ENERGIES

Various types of Coulomb effects were investigated both experimentally and theoretically in the past; some examples will be enumerated below.

Various results are available in the low (or intermediate) energy regime, up to a few GeV/nucleon. On the experimental side, studies at the LBNL Bevalac facility revealed that the Coulombic field causes extremely large effects at forward angles, i.e., at projectile velocity [7,8]. The Coulombic effect was also observed at subthreshold energies [9]. In studies of p+Au and He+Au reactions at several GeV/nucleon, the nonrelativistic approach to the Coulomb field brought precise information on the evolution of the nuclear fragmentation process [10]. Finally, an interesting charge asymmetry was

found in the kinetic energy spectrum of particles produced in collisions of 9 GeV protons with emulsion nuclei [11].

The situation on the theoretical side is rather complicated. Attempts were made to describe the intermediate energy minimum bias data by a multiparametric modeling of the pion source fireballs, and calculating the subsequent transport of pions in the Coulomb field of the spectators [12,13]. Quantal effects were discussed in Ref. [14]. Other simple models were considered in Refs. [15–17]. An interesting analysis of the influence of the electric charge on spectra of kaons produced in collisions of heavy nuclei can be found in Ref. [18].

In the higher energy regime, studies of spectator Coulomb interactions offer two advantages relative to the low energies. On the experimental side, impact parameter (centrality) selection becomes possible by produced particle multiplicity measurement or by forward calorimetry. This allows a selection of peripheral collisions where the spectator effect will be the largest. On the theoretical side, seen in the context of typical relativistic pion velocities, the breakup of the spectator system can be assumed to be slow. This simplifies the picture. However, a fully relativistic description of electromagnetic effects involving, e.g., retardation phenomena becomes a necessity at high energies.

In early cosmic ray experiments, large π^+/π^- asymmetries were observed for produced slow pions [19]. As far as nucleus+nucleus collisions and SPS energies are concerned, various experimental [20–22] and theoretical [23,24] papers on the influence of the electromagnetic field on particle production in the midrapidity ($x_F = 0$) region[1] of Pb+Pb reactions are known. However, these focus on the role played by the electromagnetic field originating from particles taking direct part in the reaction.

As far as the influence of the two spectator systems *outside midrapidity* is concerned, we are aware of only one published measurement [25], which was performed for a very limited acceptance range (forward angles, i.e., $p_T \approx 0$). New and better measurements can be expected in the future from the NA49 apparatus [26]. No theoretical description is known to us. To provide such a simplified but realistic description is the main purpose of the present paper.

III. MODELING A PERIPHERAL Pb+Pb COLLISION AT SPS ENERGIES

Our aim is to obtain a realistic estimate of the spectator-induced electromagnetic effect, avoiding, however, the discussion of complex and poorly known details of soft hadronic particle production. Thus we decide on a maximally simplified approach, illustrated in Fig. 1. A peripheral Pb+Pb reaction can be imagined to consist of three steps:

(i) The collision takes place at a given impact parameter b; the two highly charged spectator systems follow their initial path with essentially unchanged momenta.

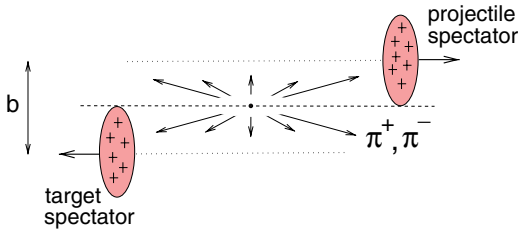

FIG. 1. (Color online) Our simplified view of a Pb+Pb collision. The hypothetical pion emission region is reduced to a single point in position space (see text).

(ii) The participating system evolves until it finally gives birth to final state pions; the evolution of the pion emission region in space and time is *a priori* unknown.

(iii) Charged pion trajectories are modified by electromagnetic interaction with the spectator charge; the spectator systems undergo a complicated nuclear fragmentation process.

We model these steps in the following simplified way:

(i) A peripheral Pb+Pb collision involving 60 participating nucleons is assumed. This corresponds to an impact parameter $b = 10.61$ fm (see Sec. III A). The two spectator systems are modeled as two uniform spheres in their respective rest frames. The sphere density is the standard nuclear density $\rho = 0.17/\text{fm}^3$. The total positive charge of each spectator system is $Q = 70$ elementary units. In the collision rest frame, the two spheres become charged disks (Fig. 1).

(ii) The pion emission region is reduced to a single point in space, namely, the original interaction point. The emission time t_E is a free parameter in our model. For the peripheral Pb+Pb reactions studied here, we assume that the initial two-dimensional (x_F, p_T) distribution of the emitted pion is similar to that in underlying nucleon+nucleon collisions.

(iii) Charged pions, with their initial momentum vector defined above in point (2), are numerically traced in the electromagnetic field of the spectator charges until they reach a distance of 10 000 fm away from the original interaction point and from each of the two spectator systems. The fragmentation of the spectator systems is neglected; the influence of participant charge, strong final state interactions, etc., are not considered.

For each of these steps, the details of our approach are explained below.

A. Collision geometry

We adjust the geometry (centrality) of the considered Pb+Pb collision to 60 participating nucleons in order to make it comparable to that of peripheral heavy ion data samples collected at the SPS [27].

The relation between the reaction impact parameter b, the number of participating nucleons N_{part}, and the spectator

[1]Note: the Feynman variable $x_F = 2p_L/\sqrt{s}$, the transverse momentum p_T, the energy E, and other related quantities will always be considered in the nucleon+nucleon c.m. system.

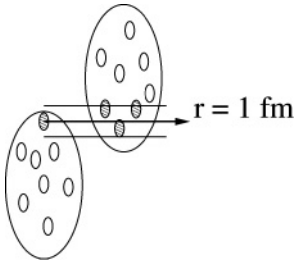

FIG. 2. Geometrical model of a Pb+Pb collision showing participating nucleons (filled ellipses) and spectator nucleons (empty ellipses).

charge Q is defined by the nuclear density profile and the elementary nucleon+nucleon cross section. We study this relation by means of a geometrical Monte Carlo simulation. This simulation (Fig. 2) produces spatial distributions of protons and neutrons using nuclear density profiles obtained for ^{208}Pb by Mizutori *et al*. in the Hartree-Fock-Bogoliubov (HFB) approach [28]. For each Pb+Pb reaction, a nucleon is defined as participant if it is crossed by one or more nucleons from the adverse nucleus within a transverse radius of less than 1 fm. This corresponds to an elementary nucleon+nucleon cross section of 31.4 mb in good agreement with experimental data [29]. No reinteraction with the spectator system is considered.

Technically, the simulation is performed at a fixed value of the impact parameter b. We obtain the average number of participants $N_{\text{part}} = 60$ at $b = 10.61$ fm. At the same time, we obtain[2] the average charge of the spectator system $Q \approx 70$ elementary units.

Another important geometry parameter to be estimated is the displacement Δb of the spectator protons' center of gravity relative to the center of gravity of the original Pb nucleus. This displacement originates from trivial geometrical reasons (Fig. 3). Our simulation gives $\Delta b = 0.76$ fm. Thus the effective distance of closest approach between the centers of gravity of the two spectator systems will be $b' = b + 2\Delta b = 12.13$ fm.

We consider that the exact shape of the spectator systems is not essential for our subsequent simulations of electromagnetic effects. For clarity, we model the two spectator systems as two homogeneous spheres with standard nuclear densities $\rho = 0.17/\text{fm}^3$ and with properly shifted centers of gravity (Fig. 1). As discussed above, the distance of closest approach of the two spheres' centers of gravity is $b' = 12.13$ fm. The total charge of each sphere is $Q = 70$ elementary units.

For the case of peripheral collisions considered here, estimates on geometry parameters may strongly rely on a proper description of the nuclear profile. Therefore, to cross-check our results, we performed an independent simulation using a different nuclear profile: a phenomenological parametrization obtained by Trzcińska *et al*. on the basis of antiprotonic atom data [31]. With respect to the Mizutori profile, the deviations

[2]The spectator charge Q is a numerical result of the simulation. It does not *a priori* follow from N_{part} due to possible neutron halo effects [30]. Our Monte Carlo takes account of these effects.

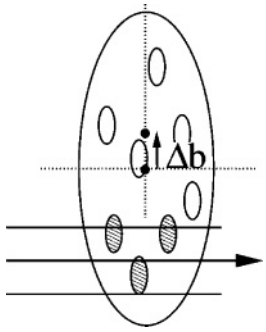

FIG. 3. As some of the nucleons become participants, the center of gravity of the spectator protons is displaced relative to the center of gravity of the original Pb nucleus.

on b', Q, and N_{part} are small and remain below 1.5%. Thus we consider our estimates as fairly precise.

B. Initial pion emission

Having established the initial geometry of the peripheral Pb+Pb reaction, we subsequently model the emission of produced π^+ and π^-.

We reduce the unknown initial emission region to a unique point in space, namely, the original interaction point (Fig. 1). We assume one emission time t_E which is a free parameter of our model; various values of t_E will be considered. Such a simplification of initial conditions gives a convenient way to estimate the dependence of the electromagnetic effect on the characteristics of the initial pion emission process (such as the pion formation time or its distance from the two spectator systems).

We assume that the initial kinematical spectra of the emitted pions are similar to those in nucleon+nucleon collisions and that they follow wounded nucleon scaling [32]. Full azimuthal symmetry of the emission is assumed. The detailed shape of the emitted pion density distribution requires an additional discussion.

A very precise and complete set of experimental data on π^+ and π^- production in p+p collisions is available at the SPS [29]. The published double differential spectra of pions in x_F and p_T display a strong dependence on pion isospin. They also contain local shape structures attributed to the production of hadronic resonances and their subsequent decay into pions. It has been demonstrated that such elementary effects reappear in nuclear collisions [4]. Any attempt at an in-depth description of Pb+Pb interactions must take them into account.

Such a description is, however, beyond our specific scope. As we concentrate on the spectator-induced Coulomb effect *per se*, we need a clear distinction between hadronic and electromagnetic phenomena to allow for an easy interpretation of our results. Thus, we simplify the situation: (1) we neglect isospin effects, i.e., assume equal initial emission spectra for π^+ and π^-; (2) we construct a smooth two-dimensional shape that reproduces the most basic features of the pion production data [29]; it does not include the more subtle, local shape structures.

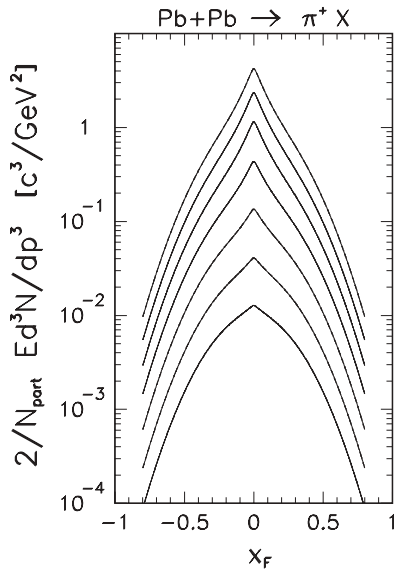

FIG. 4. Assumed invariant density of π^+ emitted per participant pair in Pb+Pb collisions, drawn as function of x_F at fixed p_T values. From top to bottom, the curves correspond to $p_T = 50$, 100, 200, 400, 600, 800, and 1000 MeV/c. For clarity, the two top curves are multiplied by 2.5 and 1.5, respectively. The invariant density of emitted π^- is assumed to be identical.

The resulting two-dimensional invariant pion density[3] is drawn in Fig. 4. We do not consider values higher than $|x_F| = 0.8$. We checked that below $p_T = 1$ GeV/c, our curves typically deviate from measured average pion ($\frac{\pi^+ + \pi^-}{2}$) densities by about 10%. Maximal deviations reach up to 21% of our assumed density. Such a gross description is sufficient for our specific aim. Evidently it cannot be used as a "fit" or "parametrization" of the data. Note that the failure of oversimplified analytical parametrizations to reproduce the $p+p$ data has been demonstrated in Ref. [29].

For completeness, we write the analytical form of our emitted pion density per participant pair as

$$\frac{2}{N_{\rm part}} E \frac{d^3N}{dp^3}_{\rm Pb+Pb\to\pi X} = \sum_{n=1,2} a_n \exp[-(x/b_n)^{c_n}] \times \exp(-u_T/d_n), \quad (1)$$

where $\pi = \pi^+$ or π^-, $N_{\rm part} = 60$ (Sec. III A), $x = \sqrt{x_F^2 + g^2}$, $u_T = \sqrt{q^2 + p_T^2}$, and numerical parameter values are listed in Table I:

C. Propagation of charged pions in the spectator electromagnetic field

The initially produced charged pions are subjected to the electromagnetic field of the two spectator systems moving at relativistic velocities.

[3]Note that in terms of x_F, p_T, and azimuthal angle ϕ, our invariant pion density per event and per participant pair writes $\frac{2}{N_{\rm part}} E \frac{d^3N}{dp^3} = \frac{2}{N_{\rm part}} \frac{2E}{p_T\sqrt{s}} \frac{d^3N}{dx_F dp_T d\phi}$.

TABLE I. Numerical parameter values.

n	a_n (c^3/GeV^2)	b_n	c_n	d_n (GeV/c)	
1	2.32229	0.369967	2.0	0.191506	$g = 0.01$
2	24.4563	0.0873833	1.001	0.12	$q = 0.334\,968$ (GeV/c)

We choose the overall center-of-mass system (c.m.s.) of the collision to calculate the evolution of pion trajectories. For symmetric Pb+Pb collisions and neglecting the Fermi motion effect (see Ref. [6]), this is also the nucleon+nucleon center-of-mass system.

We assume that for ultrarelativistic Pb+Pb reactions, the nuclear fragmentation process is slow relative to the relativistic pion velocities and can be neglected in a first approximation. Thus the spectator nucleon velocity remains constant and identical to the velocity of the parent Pb ion.

We define our space coordinate system in the way shown in Fig. 5. For simplicity, we label the two spectator systems as left (L) and right (R). We set the time scale such that at $t = 0$ the center of gravity of each of the spectator systems is found at $z_L = z_R = 0$. Thus the time-dependent position of the moving spectators is

$$\vec{R}_L(t) = -\vec{b}/2 + \vec{v}_L \cdot t, \quad \vec{R}_R(t) = \vec{b}/2 + \vec{v}_R \cdot t. \quad (2)$$

Here, $\vec{v}_L$ and $\vec{v}_R$ are the two spectator velocity vectors. For the SPS energy discussed here $v_L = v_R \equiv v_S = 0.994c$. The value of the impact parameter vector $\vec{b}$ is set to $b = 12.13$ fm (see Sec. III A).

Each of the two spectator systems defines its own rest frame. We define $\vec{E}'_L$ as the constant electrostatic field generated by the spectator L in its rest frame, and $\vec{E}''_R$ as the field generated by the spectator R in its rest frame. Having assumed both systems as uniform spheres with a normal nuclear density $\rho = 0.17$/fm^3 and with a total charge $Q = 70$ elementary units

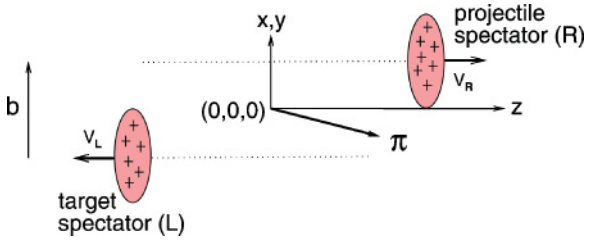

FIG. 5. (Color online) Space coordinate system for the Pb+Pb collision. The origin $(x, y, z) = (0, 0, 0)$ is located at the interaction point. Projectile and target spectators are denoted left (L) and right (R). Impact parameter $\vec{b}$ is a vector.

(Sec. III A) we write

$$\vec{E}'_L(\vec{r}'_c) = \begin{cases} kQ\ \vec{r}'_c/r'^3_c & \text{for} \quad r'_c > R_s, \\ kQ\ \vec{r}'_c/R_s^3 & \text{for} \quad r'_c < R_s, \end{cases} \tag{3}$$

$$\vec{E}''_L(\vec{r}''_c) = \begin{cases} kQ\ \vec{r}''_c/r''^3_c & \text{for} \quad r''_c > R_s, \\ kQ\ \vec{r}''_c/R_s^3 & \text{for} \quad r''_c < R_s, \end{cases} \tag{4}$$

In the equations above, $\vec{r}'_c$ ($\vec{r}''_c$) is the position relative to the center of the L (R) spectator, defined in this spectator's rest frame. $k \approx 1.44\ \text{MeV} \cdot \text{fm}/e^2$ is the electrostatic constant. $R_s = [N_{\text{spec}}/(4/3\pi\rho)]^{1/3}$ is the sphere radius defined by the number of spectator nucleons N_{spec}. For the case considered here, $R_s = 6.3$ fm.

We transform the fields $\vec{E}'_L$, $\vec{E}''_R$ to the center-of-mass system. Here, the moving spectator charge generates both electric and magnetic fields. From the general Lorentz transformation [33], we get

$$\begin{aligned} \vec{E}_L(\vec{r},t) &= \gamma_s \vec{E}'_L(\vec{r}'_c) - \frac{\gamma_s^2}{\gamma_s+1}\frac{\vec{v}_L}{c}\left(\frac{\vec{v}_L}{c}\cdot\vec{E}'_L(\vec{r}'_c)\right), \\ \vec{B}_L(\vec{r},t) &= \gamma_s\left(\frac{\vec{v}_L}{c}\times\vec{E}'_L(\vec{r}'_c)\right), \end{aligned} \tag{5}$$

for the left spectator and

$$\begin{aligned} \vec{E}_R(\vec{r},t) &= \gamma_s \vec{E}''_R(\vec{r}''_c) - \frac{\gamma_s^2}{\gamma_s+1}\frac{\vec{v}_R}{c}\left(\frac{\vec{v}_R}{c}\cdot\vec{E}''_R(\vec{r}''_c)\right), \\ \vec{B}_R(\vec{r},t) &= \gamma_s\left(\frac{\vec{v}_R}{c}\times\vec{E}''_R(\vec{r}''_c)\right), \end{aligned} \tag{6}$$

for the right spectator.

In the equations above, the γ_s factor is defined as $\gamma_s = (1 - v_s^2/c^2)^{-1/2}$. The vectors $\vec{E}_L$ ($\vec{E}_R$) and $\vec{B}_L$ ($\vec{B}_R$) are, respectively, the electric and magnetic fields generated by the left (right) spectator at the space-time position $(\vec{r},t)$. The relation between $\vec{r} = (x,y,z)$ and the spectator rest frame coordinates $\vec{r}'_c = (x'_c, y'_c, z'_c)$, $\vec{r}''_c = (x''_c, y''_c, z''_c)$ is given by the Lorentz transformation and the impact parameter vector $\vec{b} = (b_x, b_y, 0)$:

$$\begin{cases} x'_c = x + b_x/2, \\ y'_c = y + b_y/2, \\ z'_c = \gamma_s(z + v_s t), \end{cases} \quad \begin{cases} x''_c = x - b_x/2, \\ y''_c = y - b_y/2, \\ z''_c = \gamma_s(z - v_s t). \end{cases} \tag{7}$$

We now consider a charged pion emitted at time $t = t_E$ from the interaction point $\vec{r} = (0,0,0)$ with its initial momentum $\vec{p}_\pi(t = t_E)$ specified by Eq. (1) from Sec. III B. This situation is illustrated in Fig. 5. The Lorentz force acting on the pion is

$$\frac{d\vec{p}_\pi}{dt} = \vec{F}_\pi(\vec{r},t) = q_\pi\left(\vec{E}(\vec{r},t) + \frac{\vec{v}_\pi(\vec{r},t)}{c}\times\vec{B}(\vec{r},t)\right), \tag{8}$$

where q_π is the pion charge, and $\vec{E}(\vec{r},t) = \vec{E}_L(\vec{r},t) + \vec{E}_R(\vec{r},t)$ and $\vec{B}(\vec{r},t) = \vec{B}_L(\vec{r},t) + \vec{B}_R(\vec{r},t)$ are standard superpositions of fields from the two sources. The resulting pion trajectory $\vec{r}_\pi(t)$ is defined by its time-dependent velocity $\vec{v}_\pi(\vec{r},t)$ as

$$\frac{d\vec{r}_\pi}{dt} = \vec{v}_\pi(\vec{r},t) = \frac{\vec{p}_\pi c^2}{\sqrt{p_\pi^2 + m_\pi^2}}, \tag{9}$$

where m_π is the pion mass. An important feature of Eq. (8) is that it implicitly takes account of relativistic retardation effects. This feature has been explicitly demonstrated in Ref. [33].

Technically, the propagation of the pion is made by means of an iterative Monte Carlo procedure. This procedure starts at $\vec{r} = (0,0,0)$ and $t = t_E$ and calculates the Lorentz force $\vec{F}_\pi(\vec{r},t)$ and the corresponding change of pion momentum and position in small steps in time. The variable step size depends on the actual distance of the pion from the nearest spectator system. The procedure is iterated numerically until the distance of the pion from the origin $(0,0,0)$ is $r > R_{\max}$, and at the same time, the distances of the pion from the spectators in their respective rest frames are simultaneously $r'_c > R_{\max}$ and $r''_c > R_{\max}$. We found that for geometries considered in the present paper, the value of the parameter $R_{\max} = 10\,000$ fm is sufficiently large to reproduce asymptotic momenta. The procedure is *weighted*, that is, each pion is generated with its proper weight $\frac{d^2N}{dx_F\,dp_T}$ deduced from Eq. (1). After the propagation procedure is finished, the same weight is used to fill the final state pion spectra. Negatively charged pions that do not escape from the spectator potential well are rejected by our procedure and do not enter into the final state distribution.

IV. RESULTS

In this section, the results of our Monte Carlo studies are discussed.

A. Charged pion spectra

We start by estimating the influence that the spectator charge exerts on double-differential spectra of pions produced in peripheral Pb+Pb reactions. For clarity, this part of the discussion remains limited to the simplest situation where the pion emission time t_E is equal to zero (immediate pion creation). This description will be generalized in Sec. IV C by considering different t_E values.

The situation is illustrated in Fig. 6. Panel (a) shows the initial spectra of emitted pions. As explained in Sec. III B, in our simple model these spectra are identical for π^+ and π^-. The presented $\frac{d^2N}{dx_F\,dp_T}$ density distributions (scaled down by the number of participant pairs) follow directly from Eq. (1).

In Fig. 6(b), the corresponding distributions of π^+ in the final state of the Pb+Pb reaction are shown. These are obtained by our Monte Carlo simulation described in Sec. III C. It is clearly apparent that the distributions are distorted by the Coulomb repulsion between the pion and spectator charges. The effect is largest for pions moving close to spectator velocities ($x_F \approx \pm 0.15$) and at low transverse momenta ($p_T = 25$ MeV/c). Here, two deep valleys in the π^+ density are visible. A similar but smaller distortion is also apparent at $p_T = 75$ MeV/c.

An opposite distortion is present for π^- densities shown in Fig. 6(c). Negative pions are attracted by the positive spectator charge and gather at low transverse momenta close to spectator velocities. This results in the presence of two large peaks at $x_F \approx \pm 0.15$. Remnants of these peaks are apparent at $p_T = 75$ MeV/c.

Thus, the Coulomb field induced by the spectator charge at SPS energies appears strong enough to produce visible

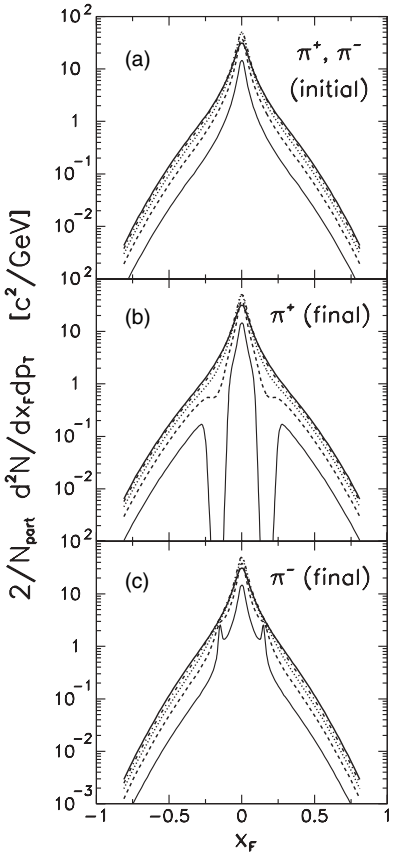

FIG. 6. Double-differential density of positively and negatively charged pions, produced per participant pair in peripheral Pb+Pb reactions. (a) Initial density of emitted π^+ and π^-. (b) Density of π^+ in the final state of the reaction. (c) Density of π^- in the final state of the reaction. In all panels, pion density is a function of x_F at $p_T = 25$ (thin solid), 75 (dash), 125 (dot), 175 (dash-dot), and 325 MeV/c (thick solid); each p_T value corresponds to a bin of ± 25 MeV/c. This simulation assumes the pion emission time $t_E = 0$. At negative x_F, reflected curves are drawn.

distortions on the pion $\frac{d^2N}{dx_F\, dp_T}$ distribution, which extends over several orders of magnitude in terms of pion density and over many GeV in terms of kinetic energy.[4]

B. π^+/π^- ratios

Further, more precise information on the spectator electromagnetic effect can be obtained by considering the density ratios of produced positive over negative pions: π^+/π^-. In our model, the π^+/π^- ratio for initially emitted pions is by definition equal to unity in the whole phase space (Sec. III B). Any deviation of this ratio from unity in the final state of the Pb+Pb reaction, therefore, directly results from the spectator-induced Coulomb interaction.

Figure 7(a) shows the x_F dependence of the π^+/π^- ratios computed for the case considered in the preceding

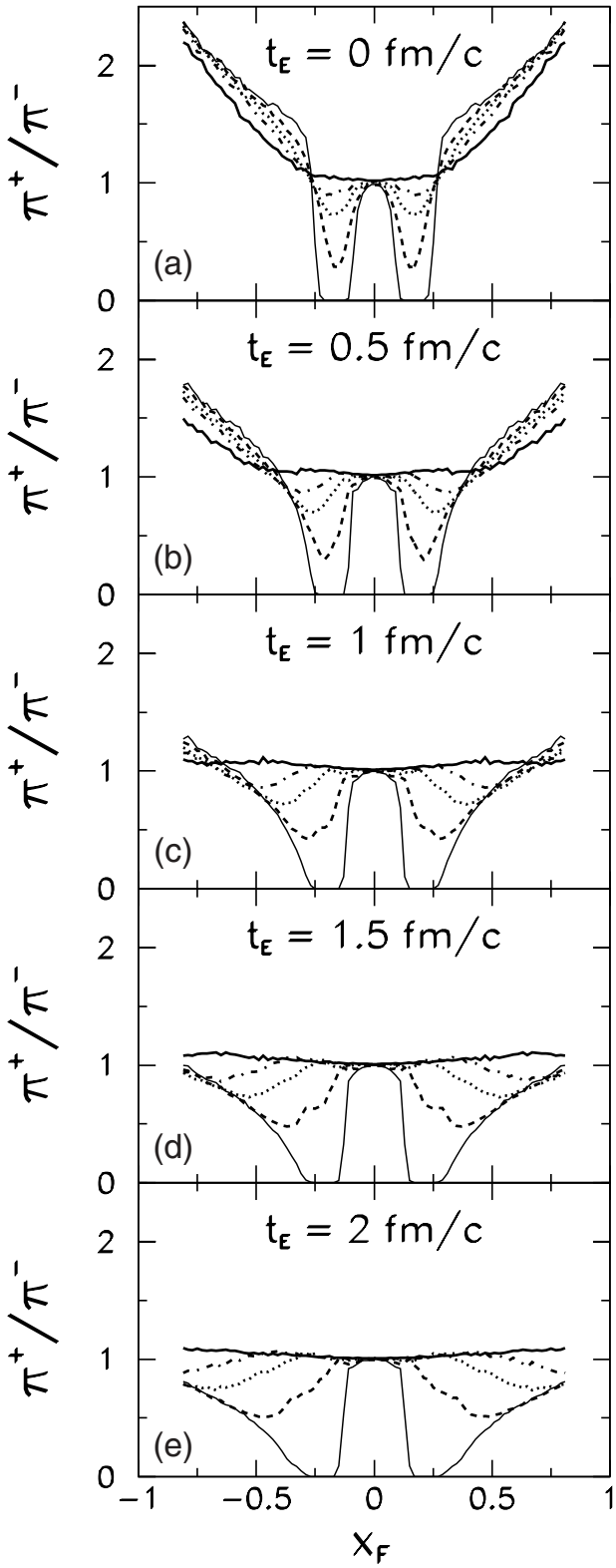

FIG. 7. Ratio of density of produced π^+ over produced π^- in the final state of the peripheral Pb+Pb reaction, obtained for five values of the pion emission time t_E. In all panels, the π^+/π^- ratio is drawn as a function of x_F at $p_T = 25$ (thin solid), 75 (dash), 125 (dot), 175 (dash-dot), and 325 MeV/c (thick solid). Small cusps on the curves correspond to the statistical fluctuations in our Monte Carlo. At negative x_F, reflected curves are drawn.

[4]In this context, it is interesting to note that the initial spectator c.m.s. electrostatic potentials induced on the pion are relatively small ($kQq/R \approx 17$ MeV for the case considered in Fig. 6).

section, namely, the pion emission time t_E assumed equal to zero. The spectator Coulomb field appears now to produce a characteristic, complex pattern of deviations from unity. The first element of this pattern is a double, two-dimensional valley which covers the low-p_T region in the vicinity of $x_F \approx \pm 0.15$; the valley remains still visible at $p_T = 175$ MeV/c. The second element is a smooth rise of the π^+/π^- ratio at higher $|x_F|$. This rise is present for all the considered p_T values; at fixed x_F, the ratio slowly decreases with increasing p_T.

C. Dependence on initial conditions

The central issue of this paper is the sensitivity of spectator-induced Coulomb effects to initial conditions of the pion production process. This issue is studied in Figs. 7(a)–7(e), where the π^+/π^- pattern obtained with the pion emission time $t_E = 0$ is compared against those computed with $t_E = 0.5$, 1, 1.5, and 2 fm/c.

Indeed, clear differences appear for different t_E values. With increasing t_E, a broadening of the double valley at $x_F \approx \pm 0.15$ and a decrease of the π^+/π^- ratio at higher absolute x_F are visible.

The study is further quantified in Fig. 8. Here, the π^+/π^- patterns obtained with different t_E values are directly compared at fixed p_T. It becomes evident that a change of 0.5 fm/c in the pion emission time is sufficient to produce visible changes in the π^+/π^- ratio. In the low transverse momentum region ($p_T < 200$ MeV/c), a displacement of the double valley toward higher absolute x_F becomes apparent on top of its broadening with t_E. At higher transverse momenta, the ratio seems to stabilize for $t_E > 1$ fm/c.

This evident sensitivity of the π^+/π^- ratio to the pion emission time t_E clearly indicates that the Coulomb effect induced by spectator protons depends on initial conditions imposed on pion production. Let us remember that in our model, the different considered values of t_E are equivalent to different distances between the pion formation zone and the two spectator systems. It can therefore be concluded that the Coulomb distortion pattern induced by spectators on π^+ and π^- spectra carries information on the evolution of the particle production process in both space and time.

D. Dependence on source size and shape

Up to now, for simplicity, we have considered only pointlike pion emission sources and discussed the relation between the time of pion emission (or, equivalently, the distance of the pion formation zone from the spectator system) and the distortion induced on final state pion spectra.

In reality, the pion emission source will be extended both in time and in space. Therefore we complete our discussion with a study of the influence of the size and shape of the pion emission source on the spectra of charged pions observed in the final state.

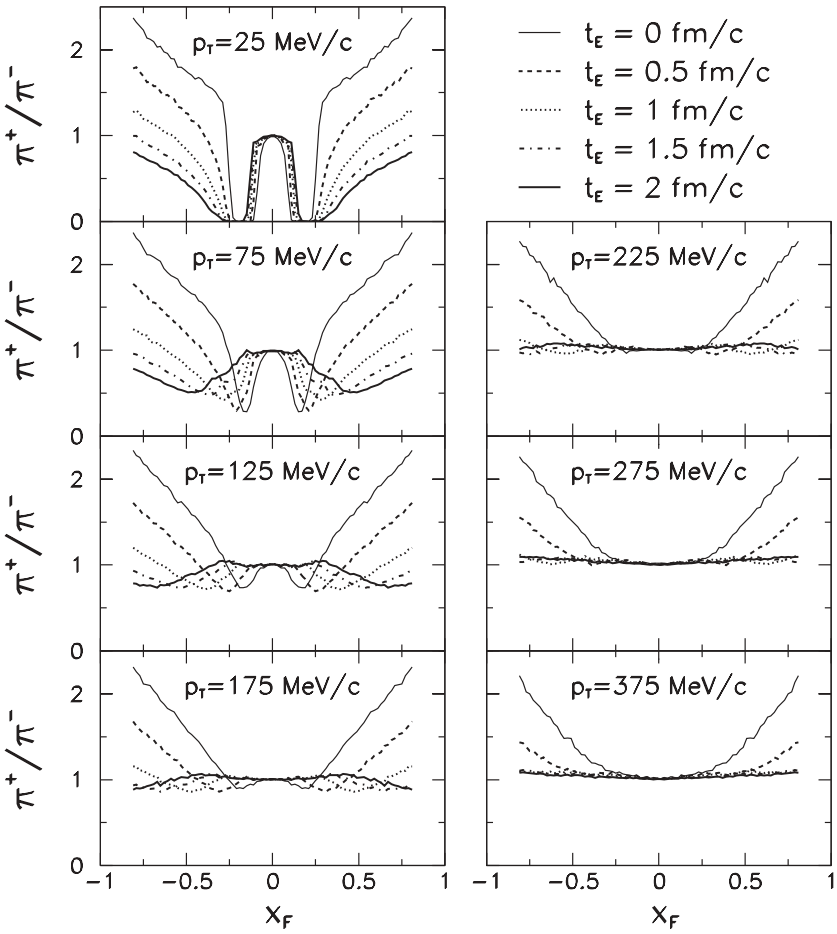

FIG. 8. Final state π^+/π^- ratio for the peripheral Pb+Pb reaction, shown at fixed values of p_T as a function of x_F. The five considered values of the pion emission time t_E are differentiated by means of different line types. At negative x_F reflected curves are drawn.

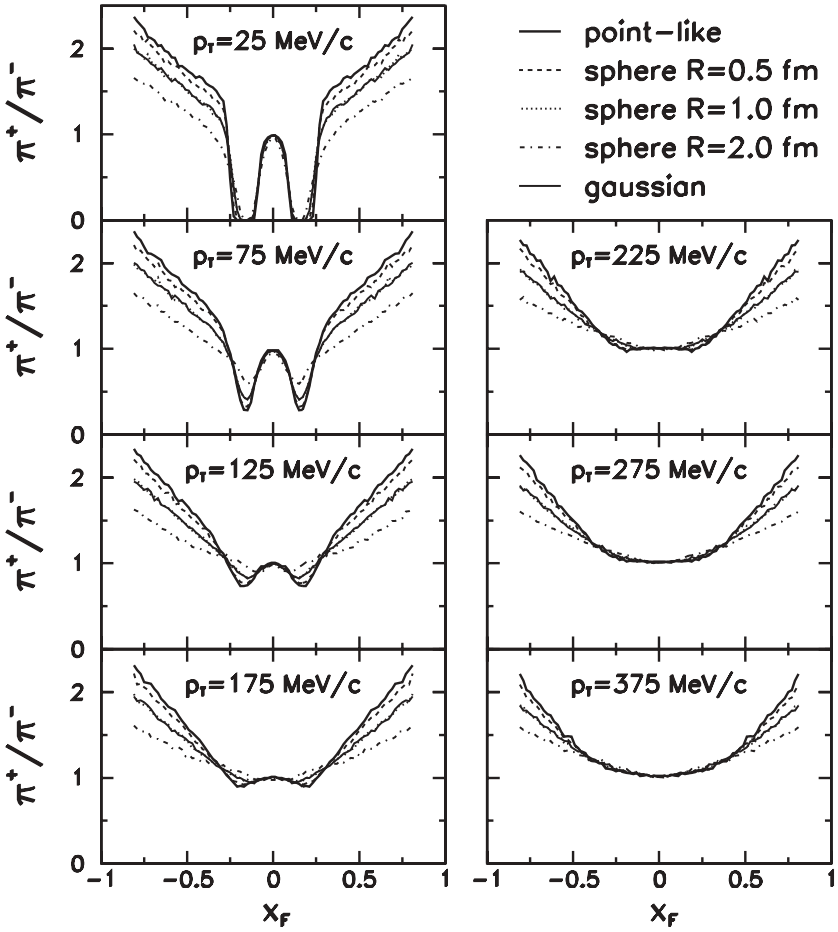

FIG. 9. Dependence of the final state π^+/π^- ratio on the size and shape of the initial pion emission zone. The π^+/π^- ratio is drawn as a function of x_F for different values of pion transverse momenta. The simulation was made assuming $t_E = 0$. The result obtained for the pointlike source is the same as in Fig. 8; the Gaussian distribution has been adjusted to match the average size of the sphere with $R =$ 1 fm (see text). At negative x_F, reflected curves are drawn.

We consider two simple shapes for the pion emission source: a uniform sphere and a three-dimensional Gaussian density distribution (cut off at three standard deviations in order to prevent too long tails which we deem unphysical). Both shapes are centered at the original interaction point $x, y, z = (0, 0, 0)$. We consider several values of the sphere radius $R = 0$, 0.5, 1, and 2 fm. For the Gaussian distribution, we consider a single value of the standard deviation which we adjust to $\sigma = 0.486$ fm; this gives the same average radius as that of the sphere with $R = 1$ fm and thus facilitates the comparison of results. For simplicity, we assume that pion emission takes place at one time t_E and neglect the possible dynamical correlations between the pion momentum and its formation time and position. We leave these items for future studies.

Figure 9 shows the influence of the source size on the final state π^+/π^- ratios, drawn as a function of x_F for different transverse momenta. The presented simulation is made assuming the pion emission time $t_E = 0$. The electromagnetic distortion induced by spectator protons appears to depend on the source size: it decreases with increasing sphere radius. This is especially visible for $|x_F| > 0.3$, i.e., outside of the characteristic Coulomb dip. On the other hand, there is no difference between the results obtained with a uniform sphere and those obtained with a Gaussian distribution, provided that the average source size is identical. We have to conclude that relative to the dominant effect of the source size, its shape has a marginal influence.

The observed source size dependence can be explained by the fact that for $t_E = 0$, the average distance between the pion formation zone and the spectator system increases with increasing source size. The fact that this dependence is weaker than that observed for emission times $t_E = 0$, 0.5, 1, and 2 fm/c (Fig. 8) can also be explained by the fact that in the latter case, this average distance is evidently larger.

We conclude that the dependence of the spectator-induced electromagnetic distortion of pion spectra on initial conditions of the pion creation process, and more specifically on the distance between the pion formation zone and the two spectator systems, results in a dependence of the above effect on first-order characteristics of the pion emission source. For the simplified case discussed here, no indication of the dependence on the source shape is seen.

V. SUMMARY AND CONCLUSIONS

The electromagnetic interaction between the spectator protons and charged pions produced in the peripheral Pb+Pb reaction has been studied by means of a simplified model. This interaction is strong enough to produce visible distortions in the final state densities of positive and negative pions.

The main feature of this "Coulomb" effect is a big dip in the π^+ density distribution at low transverse momenta in the vicinity of $x_F \approx \pm 0.15$, accompanied by an increase of π^- density in the corresponding region of phase space. This results in the presence of a double, two-dimensional valley in the π^+/π^- density ratio. At higher absolute x_F, another distortion may appear, namely, a smooth increase of π^+/π^- with x_F.

The sensitivity of this electromagnetic effect to initial conditions imposed on pion production has been estimated. The effect is clearly sensitive to initial conditions. Changes of the pion emission time by 0.5 fm/c (in c.m.s. time) are sufficient to modify the observed distortion pattern. In our model, such changes are equivalent to changes of position of the formation zone by 0.5 fm relative to the two spectator systems. Thus, the electromagnetic effect appears to depend on the evolution of the pion production process in space and time.

For extended pion emission sources, this dependence on initial conditions results in a sensitivity of the observed electromagnetic distortion of pion spectra to the size of the pion emission source. On the other hand, no indication of the dependence on the source shape is seen within the present, simplified analysis.

Our study demonstrates the importance of new, double-differential data on the (x_F, p_T) dependence of pion production in peripheral nucleus+nucleus collisions. Further analyses of this subject should take account of other effects present in nuclear reactions (multiple collisions, isospin, nuclear fragmentation, and possibly strong final state interactions of pions with the spectator systems). Also, more refined scenarios of the space-time evolution of the pion formation zone can be considered. Nevertheless, our simplified analysis clearly demonstrates that the electromagnetic phenomena induced by the presence of spectator charge carry interesting information on the mechanism of the nonperturbative particle production process. We therefore expect that future experimental pion data at SPS energies could be used to test the various existing microscopic scenarios of particle production.

ACKNOWLEDGMENTS

We wish to express our deep gratitude to Hans Gerhard Fischer for his valuable support and numerous fruitful discussions. We are especially indebted to Andrzej Górski for his careful verification of some of our results. We are greatly indebted to Dezso Varga for many inspiring remarks and for his precious help in the early stages of this work. We gratefully acknowledge Krzysztof Golec-Biernat and Jacek Turnau for discussion on some problems related to this study. This work was supported by the Polish State Committee for Scientific Research under Grant No. 1 P03B 097 29.

[1] For a review, see, e.g., K. Fiałkowski and W. Kittel, Rep. Prog. Phys. **46**, 1283 (1983).
[2] G. Baym, Acta Phys. Pol. B **29**, 1839 (1998).
[3] A. Rybicki *et al.* (NA49 Collaboration), Acta Phys. Pol. B **33**, 1483 (2002); H. G. Fischer *et al.* (NA49 Collaboration), Nucl. Phys. **A715**, 118 (2003); D. Varga *et al.* (NA49 Collaboration), Heavy Ion Phys. **17**, 387 (2003).
[4] H. G. Fischer (NA49 Collaboration), Acta Phys. Pol. B **33**, 1473 (2002); O. Chvala (NA49 Collaboration), Eur. Phys. J. C **33**, S615 (2004); A. Rybicki, Acta Phys. Pol. B **35**, 145 (2004); G. Barr *et al.*, Eur. Phys. J. C **49**, 919 (2007).
[5] P. Pawłowski and A. Szczurek, Phys. Rev. C **70**, 044908 (2004).
[6] A. Szczurek and A. Budzanowski, Mod. Phys. Lett. A **19**, 1669 (2004).
[7] W. Benenson *et al.*, Phys. Rev. Lett. **43**, 683 (1979).
[8] J. P. Sullivan *et al.*, Phys. Rev. C **25**, 1499 (1982).
[9] B. Noren *et al.*, Nucl. Phys. **A489**, 763 (1988).
[10] V. A. Karnaukhov *et al.*, Phys. At. Nucl. **69**, 1142 (2006), and references therein.
[11] E. M. Friedländer, Phys. Lett. **2**, 38 (1951).
[12] K. G. Libbrecht and S. E. Koonin, Phys. Rev. Lett. **43**, 1581 (1979).
[13] J. Cugnon and S. E. Koonin, Nucl. Phys. **A355**, 477 (1981).
[14] M. Gyulassy and S. K. Kauffmann, Nucl. Phys. **A362**, 503 (1981).
[15] A. Bonasera and G. F. Bertsch, Phys. Lett. **B195**, 521 (1987).
[16] B.-A. Li, Phys. Lett. **B346**, 5 (1995).
[17] H. W. Barz, J. P. Bondorf, J. J. Gaardhoje, and H. Heiselberg, Phys. Rev. C **57**, 2536 (1998).
[18] A. Ayala and J. Kapusta, Phys. Rev. C **56**, 407 (1997).
[19] H. Yagoda, Phys. Rev. **85**, 891 (1952).
[20] H. Boggild *et al.* (NA44 Collaboration), Phys. Lett. **B372**, 339 (1996).
[21] M. Gonin *et al.* (E802/E866 Collaboration), Nucl. Phys. **A566**, 601c (1994); H. Hamagaki *et al.* (E802/E866 Collaboration), *ibid.* **A566**, 27c (1994); F. Videbaek *et al.* (E802/E866 Collaboration), *ibid.* **A591**, 249c (1995).
[22] M. M. Aggarwal *et al.* (WA98 Collaboration), arXiv: nucl-ex/0607018.
[23] T. Osada, S. Sano, M. Biyajima, and G. Wilk, Phys. Rev. C **54**, R2167 (1996).
[24] A. Ayala, S. Jeon, and J. Kapusta, Phys. Rev. C **59**, 3324 (1999).
[25] G. Ambrosini *et al.* (NA52 Collaboration), New J. Phys. **1**, 23 (1999).
[26] Preliminary data can be found in A. Rybicki, J. Phys. G **30**, S743 (2004); O. Chvala (NA49 Collaboration), Nucl. Phys. **A749**, 304 (2005); A. Rybicki, Int. J. Mod. Phys. A **22**, 659 (2007).
[27] J. Bächler *et al.* (NA49 Collaboration), Nucl. Phys. **A661**, 45c (1999); G. E. Cooper (NA49 Collaboration), *ibid.* **A661**, 362c (1999).
[28] S. Mizutori, J. Dobaczewski, G. A. Lalazissis, W. Nazarewicz, and P. G. Reinhard, Phys. Rev. C **61**, 044326 (2000).
[29] C. Alt *et al.* (NA49 Collaboration), Eur. Phys. J. C **45**, 343 (2006).
[30] A. Trzcińska, J. Jastrzebski, P. Lubinski, F. J. Hartmann, R. Schmidt, T. von Egidy, and B. Klos, Phys. Rev. Lett. **87**, 082501 (2001).
[31] A. Trzcińska, Ph.D. thesis, Heavy Ion Laboratory, Warsaw University, May 2001, http://www.slcj.uw.edu.pl/~agniecha/phthesis_at.ps.gz (in Polish).
[32] A. Białas, M. Bleszyński, and W. Czyż, Nucl. Phys. **B111**, 461 (1976).
[33] J. D. Jackson, *Classical Electrodynamics* (Wiley, London, 1975).